Anharmonic effects in thermoelectric and 2D materials

Unai Aseguinolaza Aguirreche

Supervided by Aitor Bergara and Ion Errea

August 24, 2020

General outline

1. Thermoelectric monochalcogenides (part 1)
   - Bulk SnSe and SnS
   - Monolayer SnSe

2. 2D materials (part 2)
   - Graphene

Outline

- Introduction
- Theoretical framework
- Part 1: Thermoelectric monochalcogenides
- Part 2: 2D materials
- Conclusions

Introduction

$$ZT = \frac{S^2 \sigma T}{\kappa}, \qquad S = -\frac{\Delta V}{\Delta T}$$

Thomas Johann Seebeck
German (1770-1831)

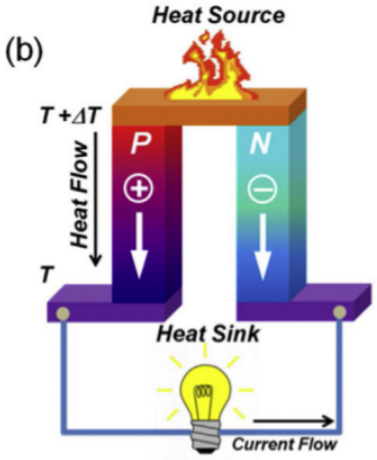

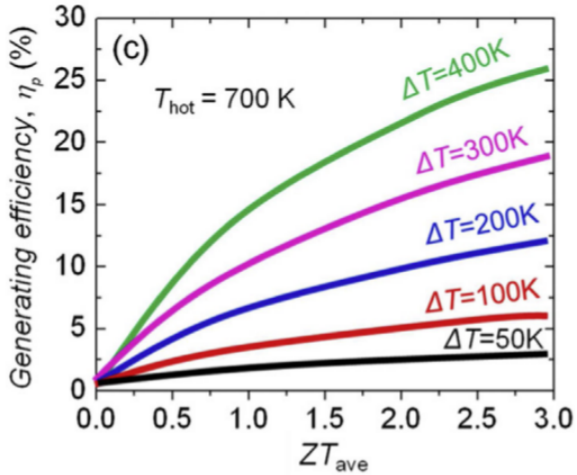

Jean Charles Athanase Peltier
French (1785-1845)

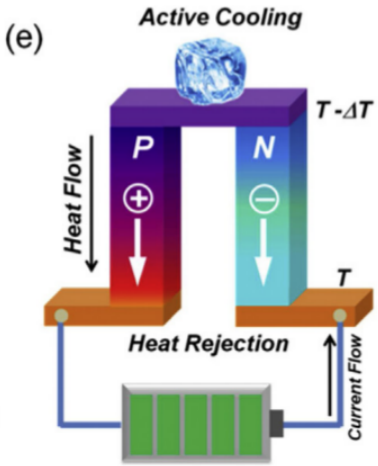

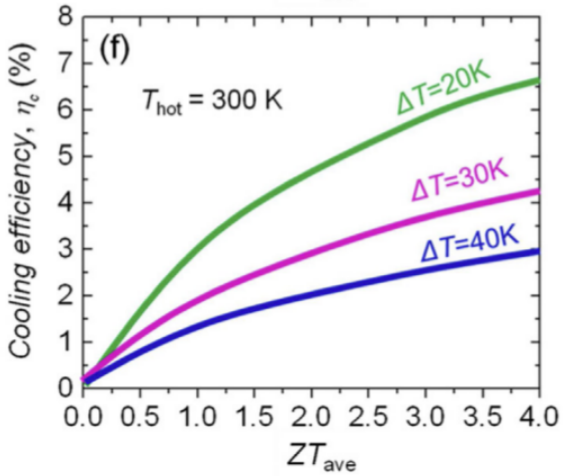

X. Zhang, L-D. Zhao / Journal of Materiomics 1 (2015) 92-105

Introduction

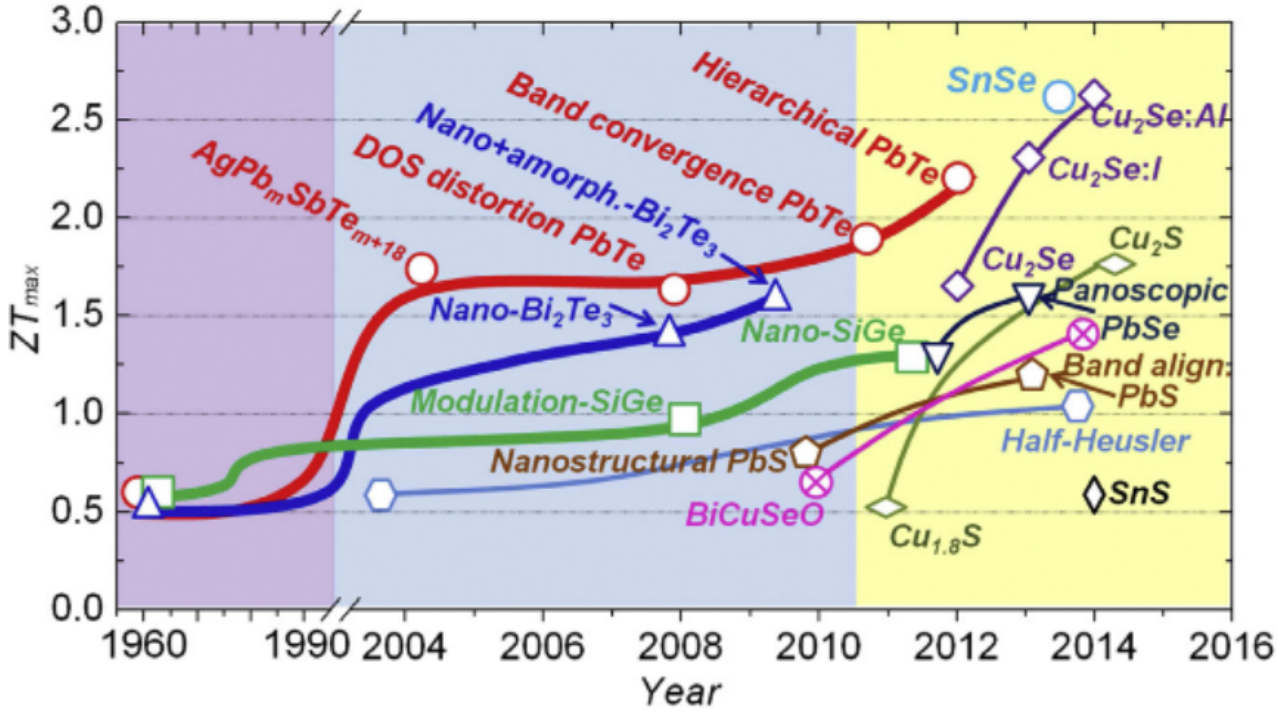

- ZT_{max} low and in narrow temperature ranges
- Very limited technological applications.

X. Zhang, L-D. Zhao / Journal of Materiomics 1 (2015) 92-105

Introduction

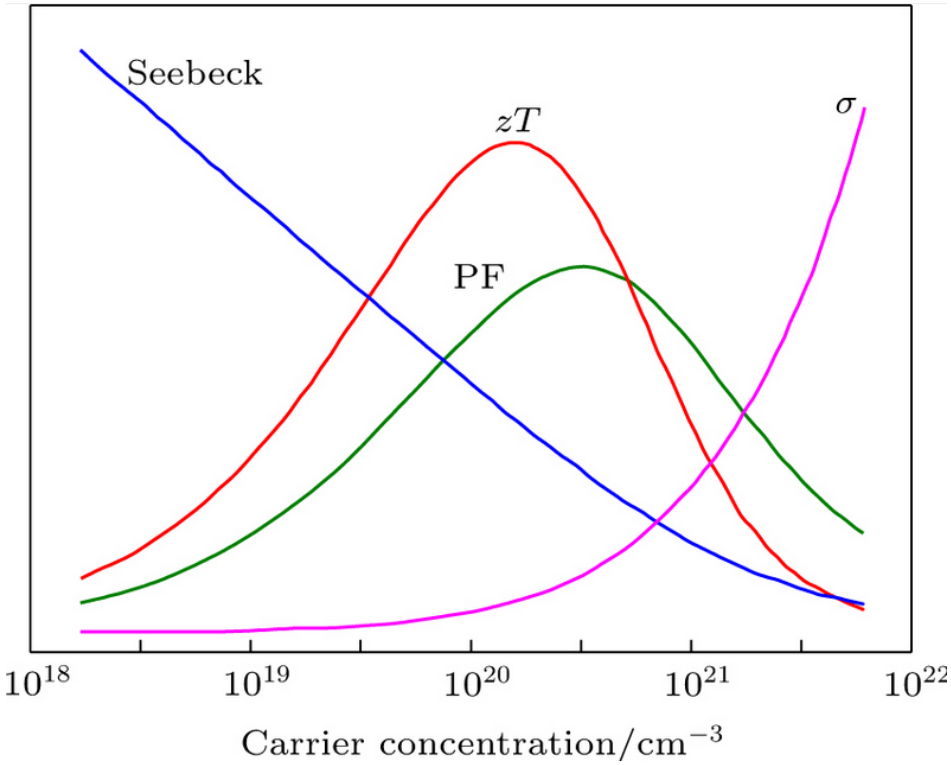

- The physical magnitudes that define ZT are correlated
- How to overcome:
  - Doping + nanostructuring
  - Proximity to phase transitions
  - ...

Introduction

LETTER

doi:10.1038/nature13184

Ultralow thermal conductivity and high thermoelectric figure of merit in SnSe crystals

Li-Dong Zhao[1], Shih-Han Lo[2], Yongsheng Zhang[2], Hui Sun[3], Gangjian Tan[1], Ctirad Uher[3], C. Wolverton[2], Vinayak P. Dravid[2] & Mercouri G. Kanatzidis[1]

The thermoelectric effect enables direct and reversible conversion between thermal and electrical energy, and provides a viable route for power generation from waste heat. The efficiency of thermoelectric materials is dictated by the dimensionless figure of merit, *ZT* (where *Z* is the figure of merit and *T* is absolute temperature), which governs the Carnot efficiency for heat conversion. Enhancements above the generally high threshold value of 2.5 have important implications for commercial deployment[1,2], especially for compounds free of Pb and Te. Here we report an unprecedented *ZT* of 2.6 ± 0.3 at 923 K, realized in SnSe single crystals measured along the *b* axis of the room-temperature orthorhombic unit cell. This material also shows a high *ZT* of 2.3 ± 0.3 along the *c* axis but a significantly reduced *ZT* of 0.8 ± 0.2 along the *a* axis. We attribute the remarkably high *ZT* along the *b* axis to the intrinsically ultralow lattice thermal conductivity in SnSe. The layered structure of SnSe derives from a distorted rock-salt structure, and features anomalously high Grüneisen parameters, which reflect the anharmonic and anisotropic bonding. We attribute the exceptionally low lattice thermal conductivity (0.23 ± 0.03 W m^{-1} K^{-1} at 973 K) in SnSe to the anharmonicity. These findings highlight alternative strategies to nanostructuring for achieving high thermoelectric performance.

power factor (along the *b* axis), but, even more surprisingly, we observe that the thermal conductivity of SnSe is intrinsically ultralow (<0.25 W m^{-1} K^{-1} at >800 K), resulting in $ZT = 2.62$ at 923 K along the *b* axis and 2.3 along the *c* axis; these represent the highest *ZT* values reported so far for any thermoelectric system. Along the *a* direction, however, *ZT* is significantly lower, ~0.8. Here, it should be noted that SnSe along the *b* axis shows a room-temperature $ZT = 0.12$, which is comparable to the room-temperature value of 0.15 reported earlier[19]. SnSe, however, reveals high *ZT* values near and above the transition temperature of 750 K at which the structure converts from *Pnma* to *Cmcm*[20–22]. Such ultrahigh *ZT* along two principal directions and the observed crystallographic and *ZT* anisotropy prompted us to investigate the scientific underpinning of these intriguing results.

SnSe adopts a layered orthorhombic crystal structure at room temperature, which can be derived from a three-dimensional distortion of the NaCl structure. The perspective views of the room-temperature SnSe crystal structure along the *a*, *b* and *c* axial directions are shown in Fig. 1a–d. There are two-atom-thick SnSe slabs (along the *b*–*c* plane) with strong Sn–Se bonding within the plane of the slabs, which are then linked with weaker Sn–Se bonding along the *a* direction[20]. The structure contains highly distorted $SnSe_7$ coordination polyhedra, which have

- The best thermoelectric material so far: Intrinsic semiconductor with low lattice thermal conductivity ($\kappa = \kappa_{el} + \kappa_l$)

Introduction

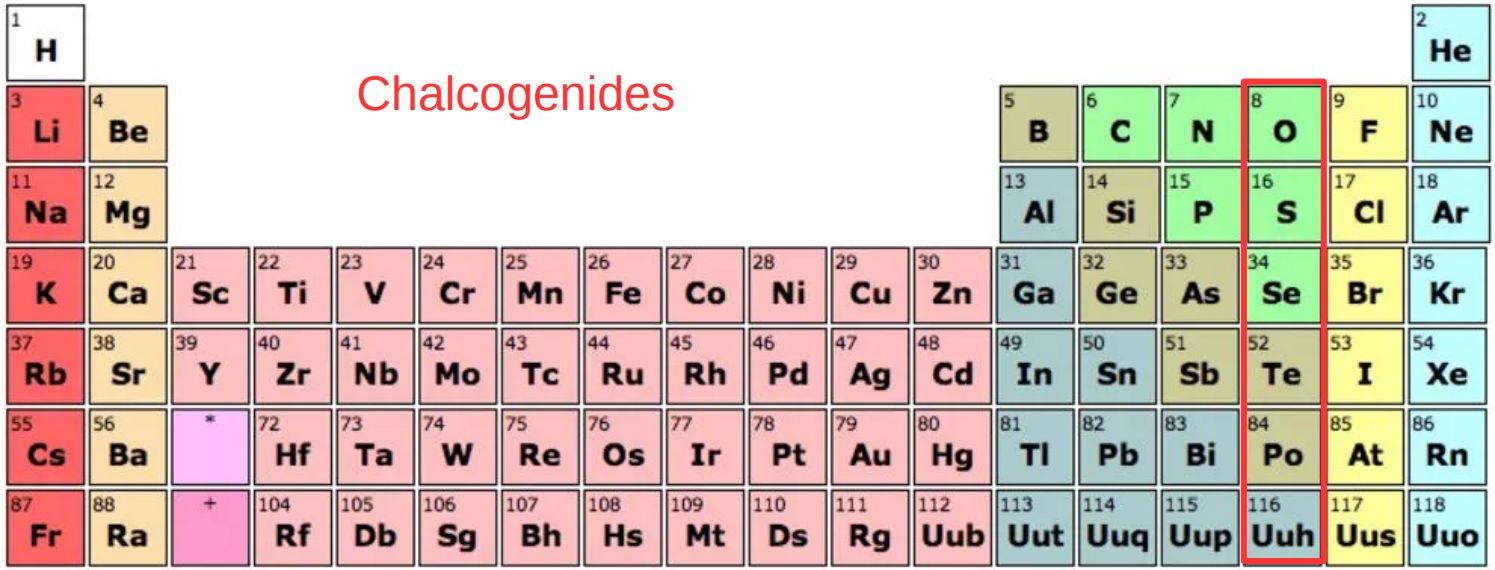

Monochalcogenides: PbTe, SnTe, GeTe, SnS...

Low lattice thermal conductivity

They show strongly anharmonic features:
- Lattice instabilities in the harmonic phonons
- Ferroelectric transitions
- Incipient ferroelectricity
- Special features in the phonon spectral function

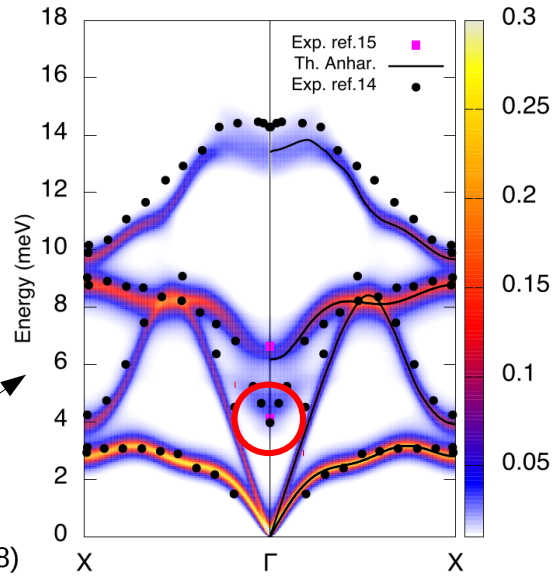

G. A. Ribeiro et al. Physical Review B 97, 014306 (2018)

Theoretical framework

- Ionic Hamiltonian

$$H = T + V(\boldsymbol{R})$$

where $\boldsymbol{R} = \boldsymbol{R}_0 + \boldsymbol{u}$.

- Assuming that $V(\boldsymbol{R})$ is well reproduced by a quadratic potential in the range of $\boldsymbol{u}$, Taylor expand the potential

$$V(\boldsymbol{R}) \simeq V(\boldsymbol{R}_0) + \frac{1}{2}\sum_{ab} \phi_{ab} u_a u_b + O(u^3)$$

where $\phi_{ab} = \partial^2 V / \partial u_a \partial u_b |_0$.

$$V^{harm}(\boldsymbol{R}) = V(\boldsymbol{R}_0) + \frac{1}{2}\sum_{ab} \phi_{ab} u_a u_b$$

- This Hamiltonian (Harmonic Hamiltonian) can be solved exactly.
- It provides well defined phonon quasiparticles

$$\sum_b \phi_{ab} \epsilon_\mu^b = M\omega_\mu^2 \epsilon_\mu^a$$

Anharmonic theory: SSCHA

- Harmonic approximation:
  - It does not work in monochalcogenides because they show harmonic instabilities.
- Perturbative approaches are not an option.
  - They are built on top of the harmonic theory.

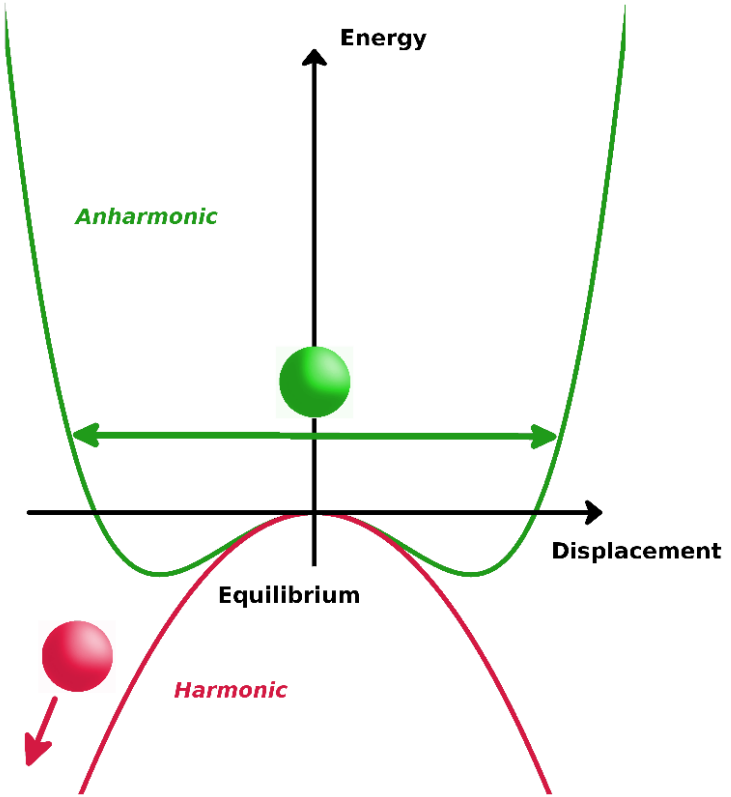

- We apply a variational non-perturbative approach with anharmonic terms to infinite order: Stochastic self-consistent harmonic approximation (SSCHA)

I. Errea et al. Physical Review Letters 111 (17), 177002 (2013) R. Bianco et al. Physical Review B 96, 014111 (2017)

Theoretical framework

- SCHA is a method for approximating the vibrational free energy of a crystal.

$$F_H = tr(\rho_H H) + \frac{1}{k_B T} tr(\rho_H ln \rho_H)$$

$$\mathcal{F}_H[\mathcal{H}] = tr(\rho_{\mathcal{H}} H) + \frac{1}{k_B T} tr(\rho_{\mathcal{H}} ln \rho_{\mathcal{H}}) = F_{\mathcal{H}} + \langle V - \mathcal{V} \rangle_{\rho_{\mathcal{H}}}$$

$$F_H \leq \mathcal{F}_H[\mathcal{H}]$$

- We take a harmonic trial density matrix $\rho_{\mathcal{H}} \equiv \rho_{\mathcal{H}}(\mathbf{\Phi}, \boldsymbol{\mathcal{R}})$. Variables $\mathbf{\Phi}$ (SCHA/auxiliary phonons) and $\boldsymbol{\mathcal{R}}$ atomic centroids.
- The SCHA provides the harmonic density matrix that minimizes the free energy.

Theoretical framework

- Landau Theory of second-order phase transitions

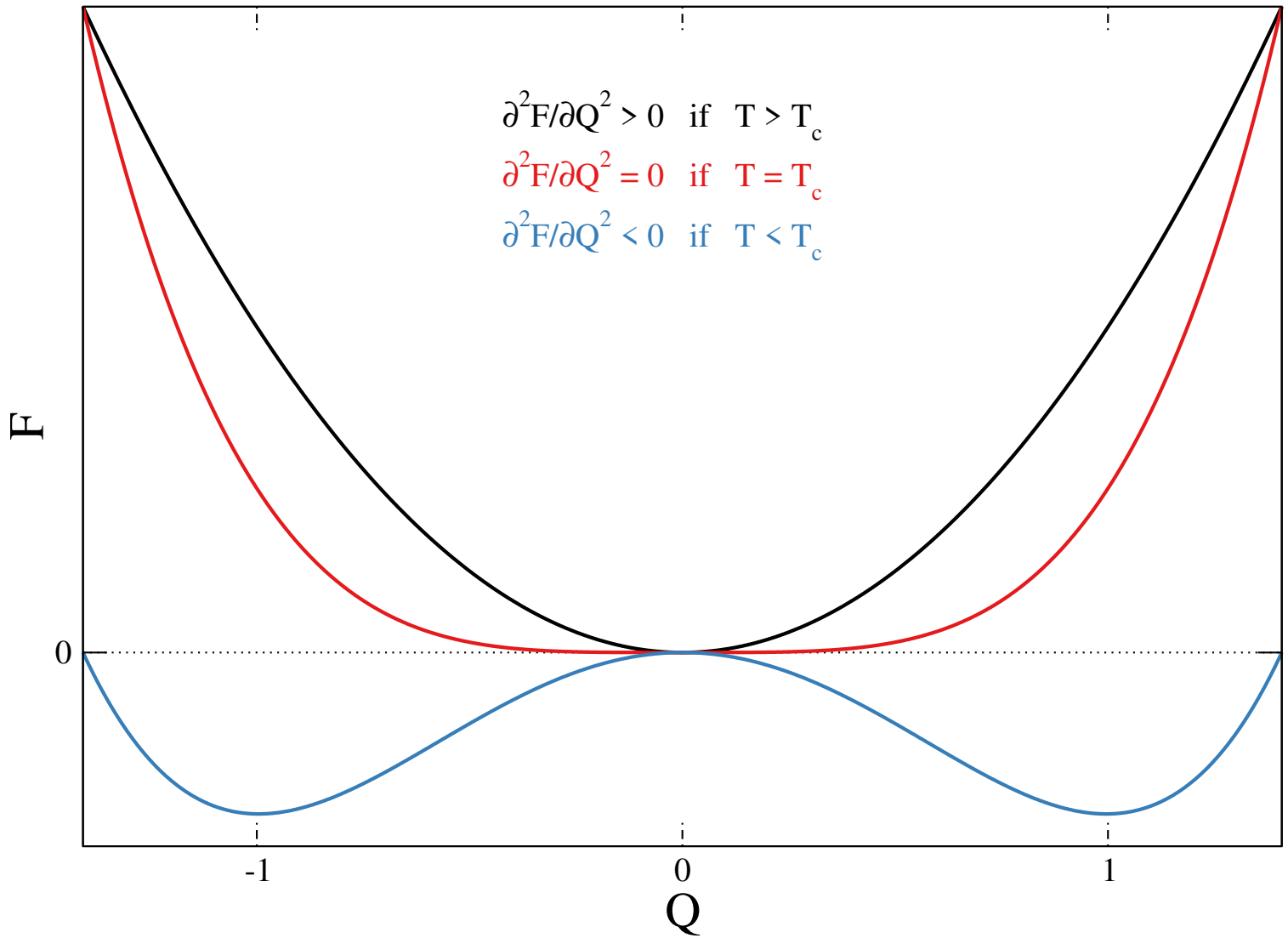

Theoretical framework

- The free energy is a well defined quantity within the SCHA.
- For a given temperature, experimentally measured phonon frequencies will be centered in the phonon frequencies defined by $\partial^2 \mathcal{F} / \partial \boldsymbol{\mathcal{R}}^2$.

$$\frac{\partial^2 \mathcal{F}}{\partial \boldsymbol{\mathcal{R}} \partial \boldsymbol{\mathcal{R}}} = \boldsymbol{\Phi} + \overset{(3)}{\boldsymbol{\Phi}} \Lambda [\mathbf{1} - \overset{(4)}{\boldsymbol{\Phi}} \Lambda]^{-1} \overset{(3)}{\boldsymbol{\Phi}}$$

- $\overset{(3)}{\boldsymbol{\Phi}} = \left\langle \frac{\partial^3 V}{\partial \boldsymbol{R}^3} \right\rangle_{\rho_{\mathcal{H}}}$, $\overset{(4)}{\boldsymbol{\Phi}} = \left\langle \frac{\partial^4 V}{\partial \boldsymbol{R}^4} \right\rangle_{\rho_{\mathcal{H}}}$, and $\Lambda \equiv \Lambda(\boldsymbol{\Phi})$.

Theoretical framework

- The static theory can be expanded by a dynamical ansatz.

$$\sigma(\mathbf{q},\omega) = \frac{1}{\pi} \times \sum_{\mu} \frac{-\omega Im\Pi_{\mu}(\mathbf{q},\omega)}{(\omega^2 - \omega_{\mu}^2(\mathbf{q}) - Re\Pi_{\mu}(\mathbf{q},\omega))^2 + (Im\Pi_{\mu}(\mathbf{q},\omega))^2}$$

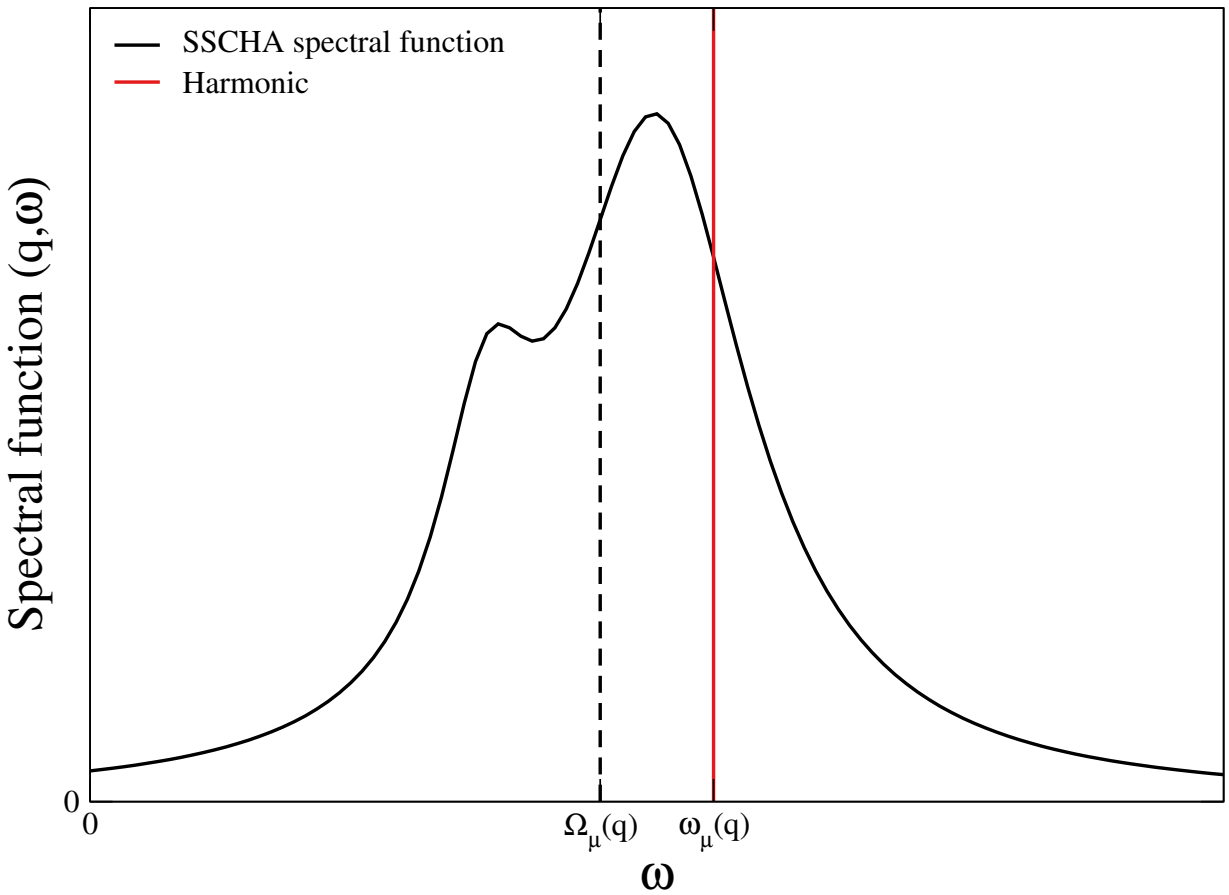

Theoretical framework

$$\mathcal{Z}_\mu(\mathbf{q},\omega) = \sqrt{\omega_\mu^2(\mathbf{q}) + \Pi_\mu(\mathbf{q},\omega + i0^+)}$$

$$\Omega_\mu(\mathbf{q}) = Re\mathcal{Z}_\mu(\mathbf{q},\omega_\mu(\mathbf{q})),$$

$$\Gamma_\mu(\mathbf{q}) = -Im\mathcal{Z}_\mu(\mathbf{q},\omega_\mu(\mathbf{q}))$$

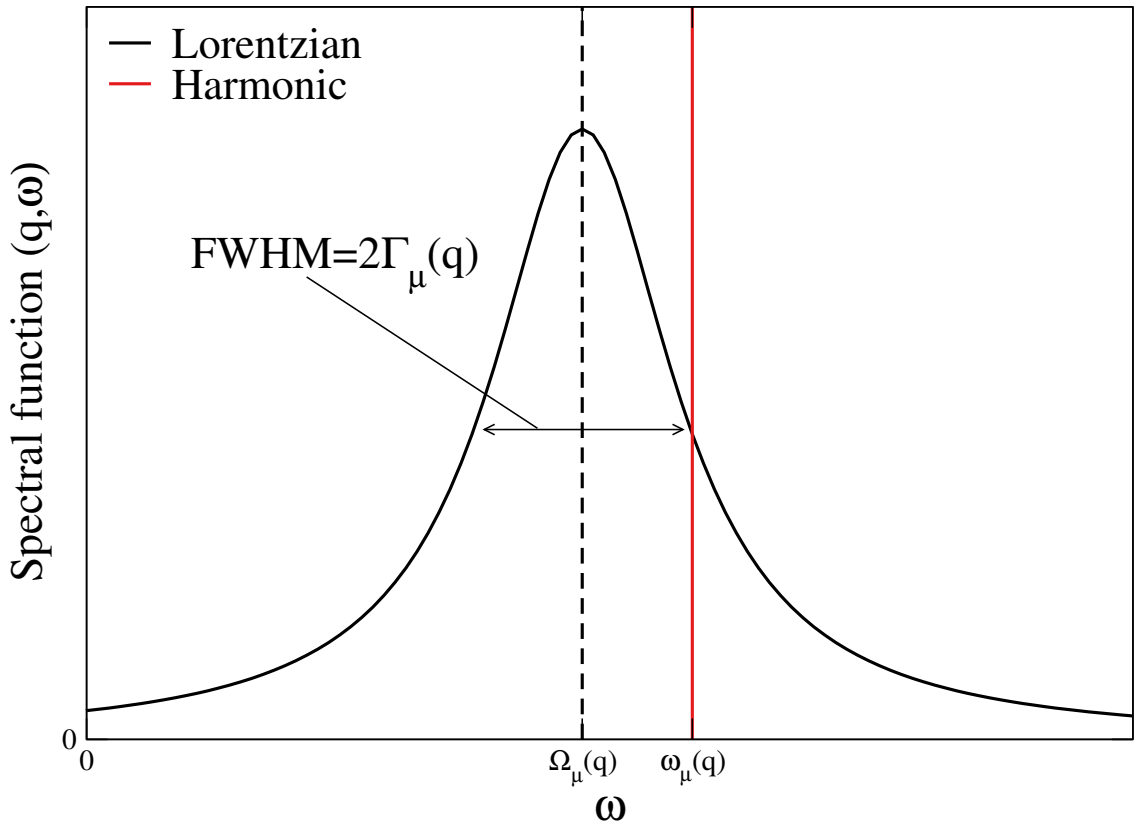

Theoretical framework

- The Lorentzian definition of phonons provides a straightforward way of calculating the lattice thermal conductivity

$$\kappa_l = \frac{1}{N_{\mathbf{q}} \Omega_{cell} k_B T^2} \sum_{\mathbf{q}\mu} v_\mu(\mathbf{q})^2 \omega_\mu(\mathbf{q})^2 n_B(\omega_\mu(\mathbf{q}))[n_B(\omega_\mu(\mathbf{q})) + 1]\tau_\mu(\mathbf{q}).$$

Summary:

- Anharmonic free energy
- Phase transition temperature
- Anharmonic phonons
- Lattice thermal conductivity

SnSe

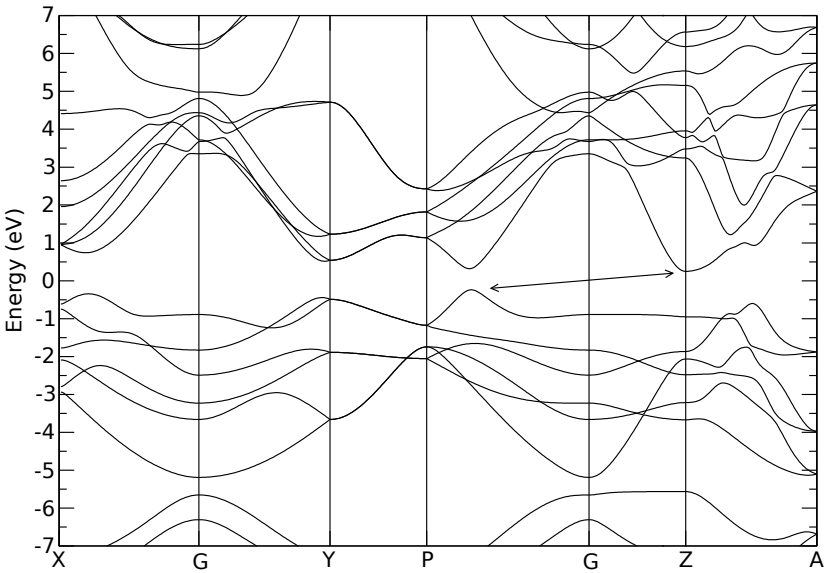

- Anisotropic crystal structure
- Narrow gap semiconductor
- Structural phase transition

Low T, low symmetry

Pnma

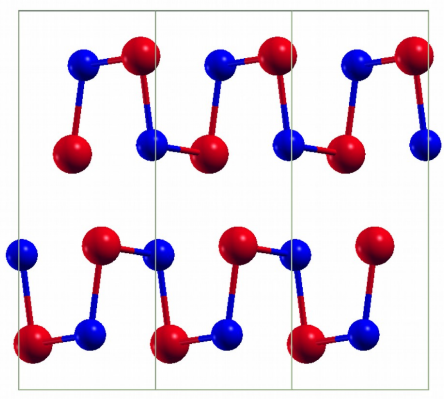

Tc = 800 K

High T, high symmetry

Cmcm

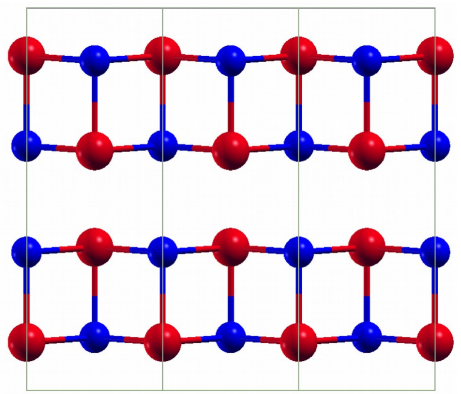

SnSe

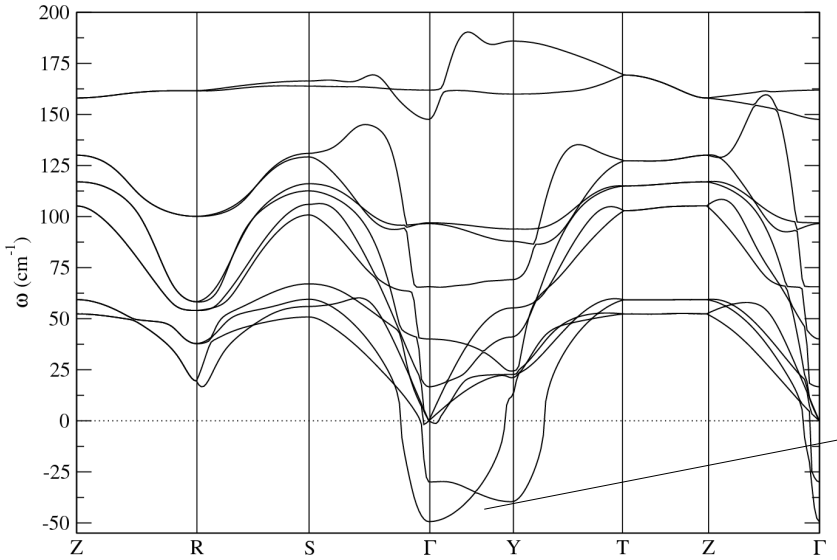

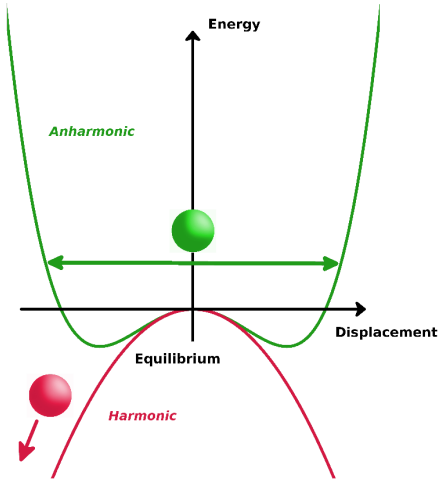

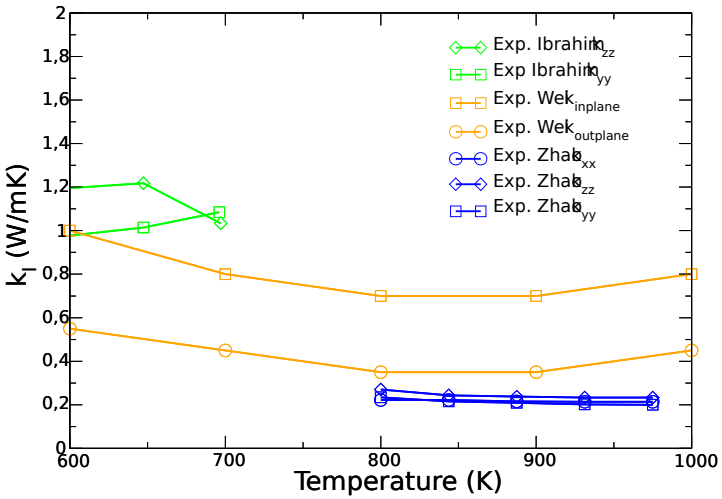

- Lattice instabilities in the harmonic approximation
- Ultralow thermal conductivity
- Experimental discrepancy
  - Value
  - Anisotropy

L.-D. Zhao et al. Nature 508, 373 (2014)

SnSe

$$\frac{\partial^2 F}{\partial Q^2} \propto \omega^2_{Y_1}(T), \quad \frac{\partial^2 F}{\partial \mathcal{R} \partial \mathcal{R}} = \mathbf{\Phi} + \overset{(3)}{\mathbf{\Phi}} \boldsymbol{W} \overset{(3)}{\mathbf{\Phi}}, \quad \overset{(3)}{\mathbf{\Phi}} = \left\langle \frac{\partial^3 V}{\partial \mathcal{R}^3} \right\rangle$$

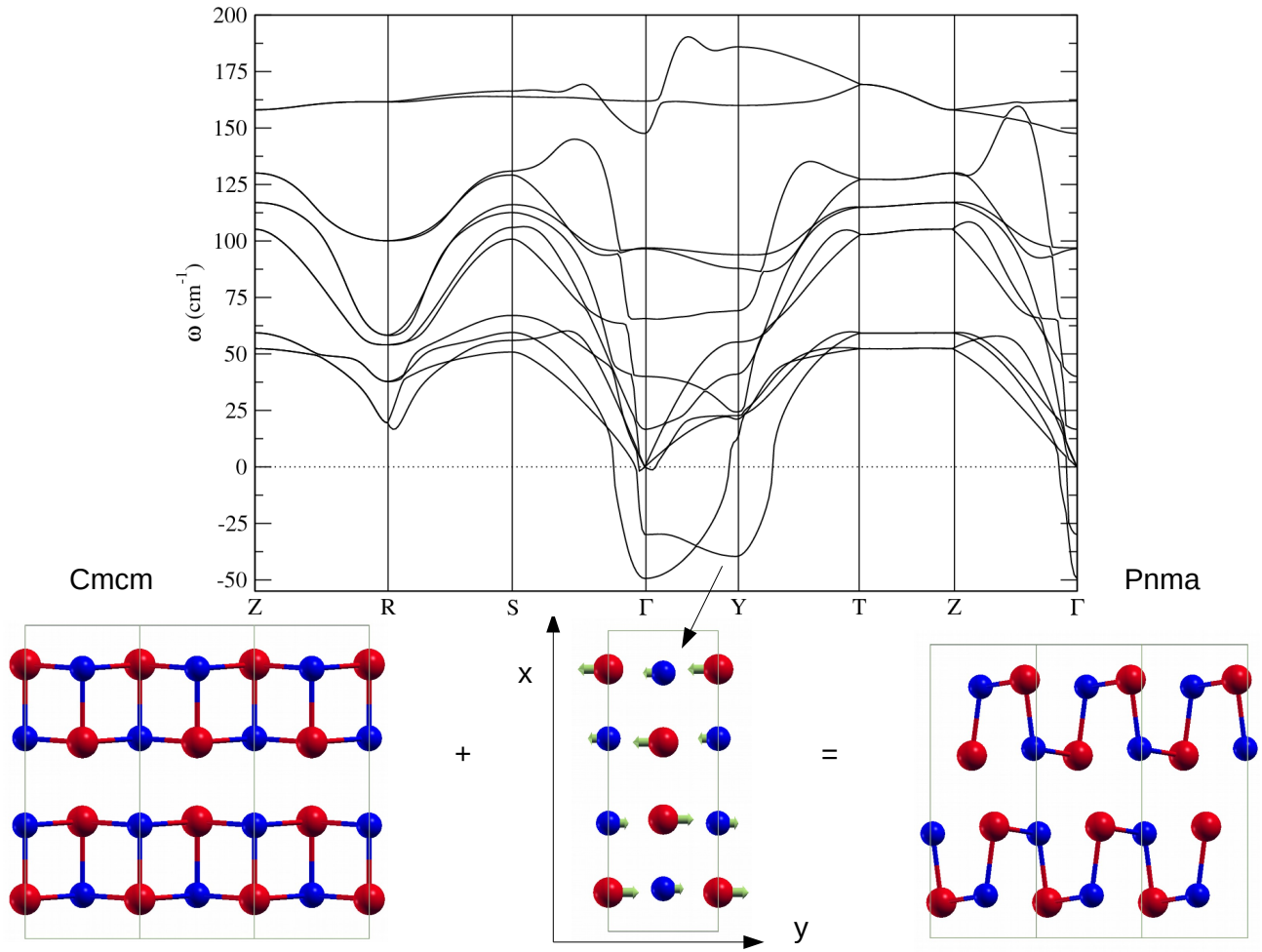

SnSe

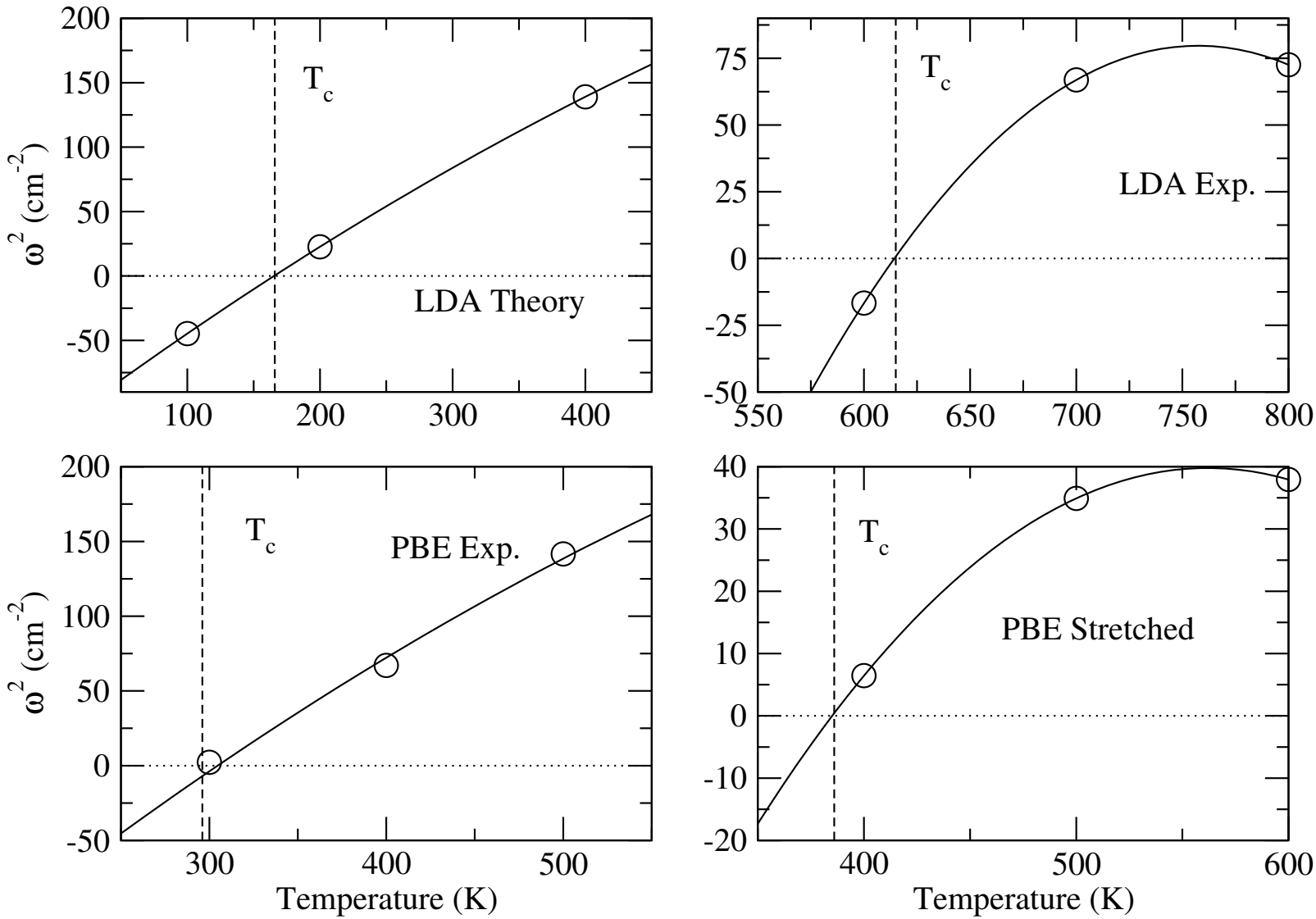
T_c
LDA Theory
LDA Exp.
PBE Exp.
PBE Stretched
ω^2 (cm^-2)
Temperature (K)

SnSe

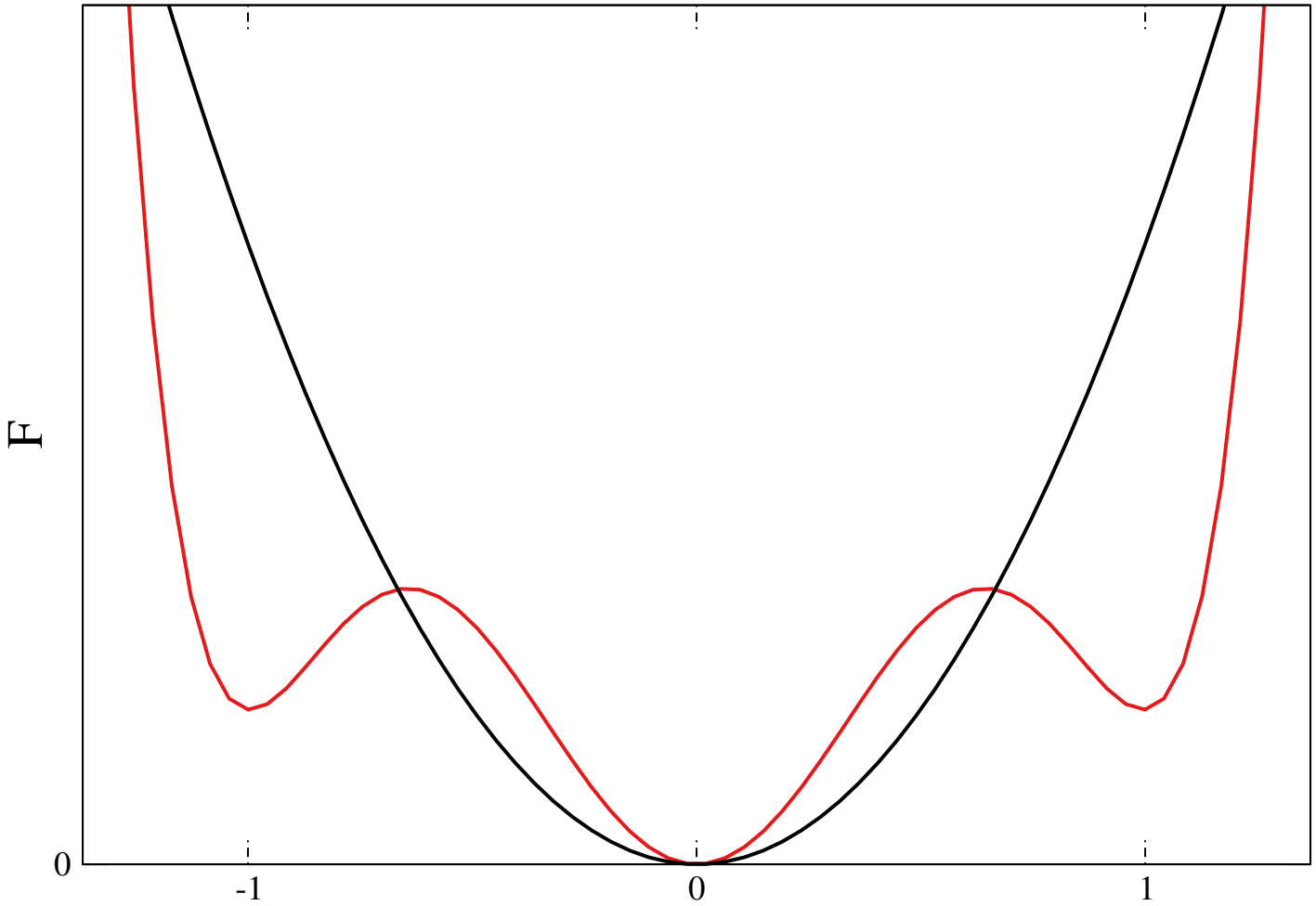

- We discard the first-order phase transition.